

# KVComp: A High-Performance, LLM-Aware, Lossy Compression Framework for KV Cache

Bo Jiang

Temple University  
Philadelphia, PA, USA  
jiang.bo@temple.edu

Chengming Zhang

University of Houston  
Houston, TX, USA  
czhang59@Central.UH.EDU

Taolue Yang

Temple University  
Philadelphia, PA, USA  
taolue.yang@temple.edu

Youyuan Liu

Temple University  
Philadelphia, PA, USA  
youyuan.li@temple.edu

Xubin He

Temple University  
Philadelphia, PA, USA  
xubin.he@temple.edu

Sian Jin

Temple University  
Philadelphia, PA, USA  
sian.jin@temple.edu

## Abstract

Transformer-based large language models (LLMs) demonstrate impressive potential in various practical applications. However, long context inference poses a significant challenge due to the enormous memory requirements of the key-value (KV) cache, which can scale to multiple gigabytes as sequence length and batch size increase. In this paper, we present KVComp, a generic and efficient KV cache management framework optimized for long-text generation that synergistically works with both latency-critical and throughput-critical inference systems. KVComp employs novel lossy compression techniques specifically designed for KV cache data characteristics, featuring careful co-design of compression algorithms and system architecture. Our approach maintains compatibility with the growing nature of KV cache while preserving high computational efficiency. Experimental results show that KVComp achieves on average 47% and up to 83% higher memory reduction rate compared to existing methods with little/no model accuracy degradation. Furthermore, KVComp achieves extremely high execution throughput, effectively reducing decompression overhead and, in some cases, even accelerating the matrix-vector multiplication operation and outperform cuBLAS-based attention kernels with less data movement.

## CCS Concepts

- Computer systems organization → Embedded systems; Redundancy; Robotics;
- Networks → Network reliability.

## Keywords

Lossy Compression, KV Cache, Large Language Model

### ACM Reference Format:

Bo Jiang, Taolue Yang, Youyuan Liu, Chengming Zhang, Xubin He, and Sian Jin. 2025. KVComp: A High-Performance, LLM-Aware, Lossy Compression Framework for KV Cache. In *Proceedings of XXXX (XXXX '25)*. ACM, New York, NY, USA, 11 pages. <https://doi.org/XXXXXX.XXXXXXX>

## 1 Introduction

Transformer-based large language models (LLMs) have revolutionized natural language processing, enabling breakthroughs in diverse tasks[4, 30]. The self-attention mechanism allows models

to capture long-range dependencies and contextual information. However, these capabilities come at a significant computational and memory cost during inference with long input contexts, where the memory footprint of the key-value (KV) cache becomes a major bottleneck[15, 24].

The KV cache stores intermediate key and value tensors for each token processed by the model and is reused during subsequent decoding steps to avoid redundant computation. As sequence length and batch size increase, the cache size grows linearly and can consume a substantial portion of GPU memory, sometimes exceeding the memory footprint of the model weights themselves[19]. For example, LLaMA2-30B inference with a context length of 32,000 and a batch size of 8 can produce over 100 GB of KV cache, surpassing the model size itself (i.e., 60 GB in float16). This growing footprint severely constrains the inference performance, limiting the achievable context length, reducing batch size, or impeding the deployment of LLMs on memory-constrained hardware[15, 19].

To address these challenges, recent studies mainly leverage three approaches to reduce KV cache size: quantization, pruning, and GPU-CPU migration. Quantization-based methods[10, 20], such as KIVI, aim to carefully design quantization strategies that minimize the impact on model accuracy. However, these techniques often achieve modest compression ratios unless combined with additional encoding, which introduces overhead and limits their applicability in latency-sensitive LLM inference. Pruning-based methods[34, 37], such as Q-Hitter, selectively discard KV pairs that are predicted to be unimportant for future decoding. While effective in some cases, these methods can suffer from unpredictable attention callbacks, leading to either costly KV recomputation or substantial accuracy degradation. GPU-CPU migration is a traditional approach for handling memory overflows, offloads KV cache data to CPU memory[27]. Although this mitigates GPU memory pressure, it significantly degrades inference performance due to data transfer latency and complex scheduling overhead.

In this paper, we present KVComp, a high-performance, LLM-aware lossy compression framework tailored for KV cache during inference. KVComp combines error-controlled quantization with GPU-based high-throughput entropy encoding and cache-resident decompression to deliver significant memory savings while preserving computational efficiency. By co-designing the compression pipeline and system-level execution, KVComp enables decompressed data to be consumed in situ within GPU shared memory

or registers, thereby avoiding global memory writeback and maximizing throughput. Our high-throughput design makes KVComp capable for deployment in LLM inference with minimum overhead. Note that our approach is orthogonal to existing pruning techniques and GPU-CPU migration strategies.

Our key contributions are as follows:

- (1) We introduce a system-aware lossy compression pipeline based on a 2D blockwise design, combining fine-grained quantization with GPU-efficient Huffman encoding to strike a balance between compression ratio and model accuracy.
- (2) We implement a cache-resident decompression solution, which is high-throughput, branch-divergence-free decompression method that fuses decoding with matrix-vector multiplication, eliminating unnecessary memory transfers.
- (3) We integrate KVComp with three LLMs and evaluate its accuracy across two benchmarks for LLM inference. Our results demonstrate up to 83% improvement in compression ratio over state-of-the-art quantization methods, with negligible or no degradation in accuracy. Moreover, KVComp achieves exceptionally high execution speed, effectively hiding decompression overhead and, in some cases, even accelerating the matrix-vector multiplication operation to outperform cuBLAS-based attention kernels.

The rest of this paper is organized as follows: Section 2 provides a background on LLM inference, lossy compression, and GPU architecture. Section 3 presents the design of our KVComp framework. Section 4 details our experimental evaluation and analysis. Lastly, Section 5 concludes the paper and future research directions.

## 2 Background and Motivation

### 2.1 Large Language Model Inference

LLMs have become foundational in natural language processing, demonstrating remarkable capabilities in tasks such as text generation[1]. The inference process for these models, particularly for generating long sequences of text (i.e., long context inference), typically involves auto-regressive decoding. In this process, the model generates output tokens one by one, with each new token depending on the previously generated ones and the initial input prompt[25, 32].

The core component of the Transformer architecture enabling this process is the attention mechanism.[32] During inference, intermediate states known as the Key (K) and Value (V) tensors are computed for each token within the self-attention layers. These K and V tensors can be reused for processing future tokens and are collectively referred to as the KV cache[26]. This cache is crucial because it allows the model to efficiently attend to relevant parts of the preceding sequence without recomputing these states for every new token generation step. The KV cache typically has a structure represented as  $[context\_len, head\_num, head\_dim]$ , where  $context\_len$  is the sequence length so far,  $head\_num$  is the number of attention heads, and  $head\_dim$  is the dimension of each head.

KV cache mainly participate in two stages[2] during inference:

**Prefill Stage:** The initial user prompt is processed in parallel by the model. This stage generates the initial KV cache based on the prompt. Shown in figure 1a. **Decode Stage:** The model generates subsequent tokens auto-regressively. In each step, a new token

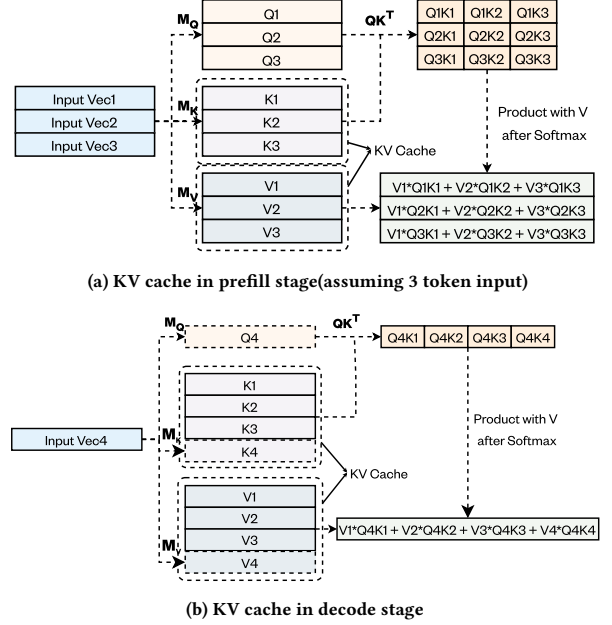


**Figure 1: KV Cache behavior during LLM Inference**,  $M_{Q,K,V}$  is the mapping matrix to  $K, Q, V$  vector. Each  $Q$  vector perform dot product with every  $K$  vector to generate a *weight* after softmax operation for each  $V$  vector. All the  $V$  vectors multiplied with their *weights* and aggregate to a output vector *Attn Output*.

is produced, its corresponding KV vectors are calculated and appended to the existing KV cache, and the entire updated cache will be used to generate the next token. This stage typically involves matrix-vector multiplications using the KV cache within the attention mechanism. Shown in figure 1b.

The KV cache is essential for avoiding redundant computation and allows efficient inference within a reasonable response time. However, it also introduces high memory consumption. As the generated sequence length  $context\_len$  and batch size increase, the KV cache grows linearly in size, potentially consuming as much or even more GPU memory than the model weights themselves[15, 19]. This large memory footprint can become a major bottleneck, limiting the maximum sequence length and batch size, degrading inference performance, or even preventing inference on hardware with constrained memory resources[15, 19]. This memory challenge motivates the development of techniques to manage the KV cache efficiently. KV cache quantization has been widely explored in recent studies[10, 20]. However, without high-speed entropy-based encoding, quantization alone offers only limited data reduction to preserve accuracy. GPU-CPU data migration, also known as offloading, is another approach to reduce GPU memory consumption by utilizing the CPU memory pool[27]. While it mitigates the risk of GPU memory overflow, it introduces significant performance overhead due to data transfer latency and complex scheduling.

### 2.2 Lossy Compression

In large neural networks, particularly LLMs, lossy compression can be applied to large data structures like activations or caches to mitigate memory bottlenecks[3, 8, 9, 12–14]. For example, quantization is a form of lossy compression that reduces the precision

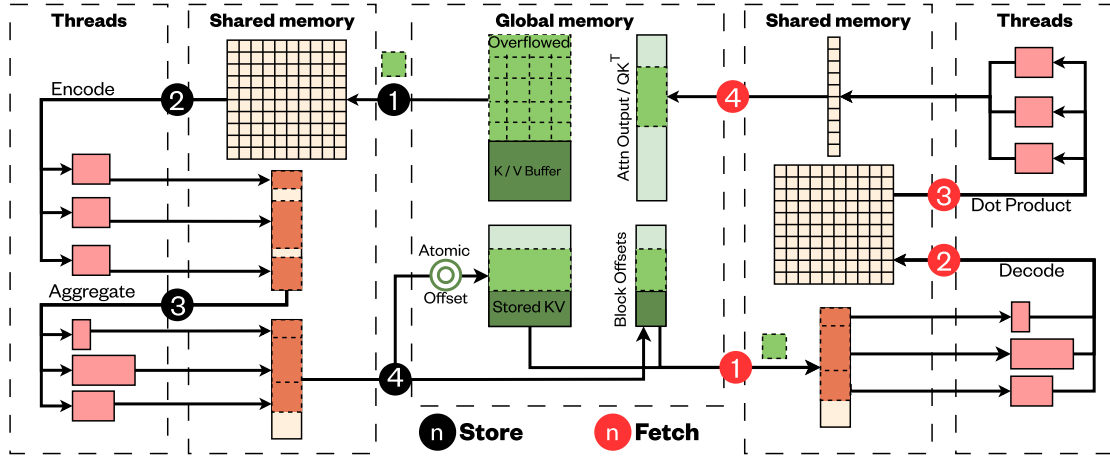


**Figure 2: Overview of KVComp.** *Store (black nodes):* 1. Load truncated 2d block to shared memory. 2. Launch threads to encode the vector for each KV vector, write the result to the thread’s buffer. 3. Aggregate all encoded bits to a whole chunk of bits. 4. Update the atomic buffer offset, write the chunk to the compressed data buffer and the offset of the chunk to the block offsets array. *Fetch (red nodes):* 1&2. Reverse operation of 3 and 4 in store. 3. With the decoded 2d block in shared memory, each thread takes responsibility for one dot product and write the result back to global memory for LLM Inference. 4. Efficiently write matrix vector multiplication result back to GPU global memory.

of numerical data by mapping continuous or high-precision values (e.g., float32) to a smaller, discrete set of values such as integers. In fact, this inherently reduces the entropy of the data, making it smaller and often more amenable to entropy encoding. In image, video, and scientific lossy compression, entropy encoding and spatial encoding are commonly added to further reduce data size[6, 6, 16, 17, 23, 28, 29, 33]. However, the low throughput of these post-quantization encoders makes them impractical for real-world LLM inference, where latency is critical. For example, CacheGen[18] integrates such encoders into the quantization pipeline and achieves throughput below 1 GB/s, which is an improvement over network transmission, but insufficient compared to the performance of GPU-CPU memory migration.

Another challenge in applying lossy compression is to manage the trade-off between the desired compression ratio and the potential impact on model accuracy. Applying quantization requires careful consideration of the data’s characteristics and the specific downstream task. Different quantization strategies, such as varying granularity (e.g., token-wise, channel-wise, block-wise) or using adaptive error bounds, can be employed to control the information loss and minimize accuracy degradation [20].

### 2.3 GPU architecture

The GPU memory hierarchy plays a crucial role in performance optimization[22]. Global memory provides the largest capacity with high latency, making efficient access patterns essential. For example, coalesced memory access can significantly improve bandwidth utilization. While shared memory in each SM is a programmer-managed cache shared among threads within a block.

GPU execution follows a Single Instruction, Multiple Thread (SIMT) model, where threads within a warp (typically 32 threads) execute the same instruction in lockstep. This model creates challenges when threads need to follow different execution paths, which is also called branch divergence that forces serialization and reduces

performance. To coordinate among threads, GPUs provide atomic operations that ensure read-modify-write sequences complete without interference, essential for managing shared resources or global indices across thread blocks.

## 3 Design Methodology

This section presents our lossy KV cache compression framework designed for large language model generative inference. Figure 2 presents an overview of the proposed framework, which is organized into two stages: **1–4 (Store)** and **1–4 (Fetch)**.

During the **Store** stage, including the LLM inference prefill phase, the KV cache generated from processing the user prompt is immediately compressed in a 2D blockwise manner to significantly reducing its memory footprint. During the subsequent decode phase, newly generated KV cache vectors are accumulated in a fixed-size buffer. Once the buffer overflows, the compressor segments the buffer into 2D blocks, compresses these blocks, and appends the compressed data to the previously stored KV cache as described in Section 3.2.3. Specifically, ①, once the buffer exceeds its optimal size, we segment its contents in place into integer multiples of the block size. For each 2D block, we assign a GPU thread block to efficiently load the data into shared memory and perform quantization in situ. ②, based on the requirements of matrix-vector multiplication, each thread encodes a slice of the 2D block residing in shared memory, storing the resulting bits in the thread’s buffer. ③, threads aggregate these encoded data within shared memory. ④, all threads cooperatively write the compressed data back to a contiguous region in GPU global memory. To prevent write conflicts, a global atomic variable governs the write-back offset. Furthermore, the compression thread block records this offset in a *Block Offsets Array* to facilitate subsequent retrieval during the **Fetch** stage.

We propose a novel quantization–entropy-encoding pipeline for compressing the KV cache. Specifically, we preallocate a dedicated buffer for each layer’s KV cache to maintain newly generated cache

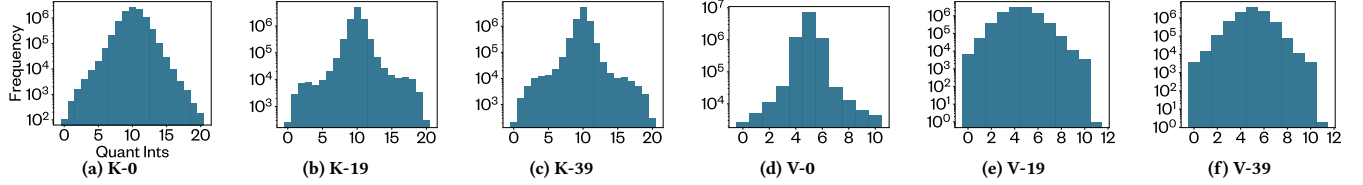


**Figure 3: Histogram of quantized KV cache based on GSM8k benchmarking of Llama2-13b. K values are block-wise quantized, while V values are token-wise quantized.**

vectors until the buffer reaches suitable size for compression. Then, we take advantage of the statistical properties of the KV cache by carefully selecting quantization units and applying quantization with a fixed relative error bound, which translates into an absolute error bound for each unit. Next, we generate the histogram of quantization codes on the GPU and construct shared Huffman codebooks on the CPU. Note that these codebooks are generated once during the prefill stage and reused during runtime, avoiding repeated overhead. Finally, we encode the quantized KV cache using our high-throughput, GPU-optimized entropy encoder.

During the **Fetch** stage, our framework adopts a just-in-time approach to minimize decompression overhead during inference. It is important to note that data flow during the **Fetch** stage is significantly more intensive than during the **Store** stage: each KV vector is compressed and stored only once but is fetched multiple times for newly generated token. Thus the decompression and memory access pattern dominate the overall performance impact, making them the primary targets of optimization in our design. Specifically, ①, we launch GPU thread blocks independently for each 2D block, loading compressed data into shared memory using the *Block Offsets Array*. ②, each thread decompresses a slice of data, mirroring the assignment from the **Store** stage. ③, dequantization is performed, and the resulting data is immediately used for dot product computations in GPU registers and shared memory as appropriate. This design minimizes global memory accesses and accelerates both decompression and attention operations. ④, shared memory serves as a buffer to write the results of matrix-vector multiplications efficiently.

### 3.1 Compression Overview

Our compression pipeline comprises two main components: **Lossy Compression via Quantization**: This step reduces data entropy by mapping high-precision values to a finite set of discrete integers. **Lossless Compression via Entropy Encoding**: the quantization codes are encoded using high-throughput GPU-optimized encoding.

**3.1.1 Quantization.** Quantization is the only lossy step in our compression pipeline that may impacts model accuracy. Consequently, our method achieves same accuracy to that of standalone quantization while providing additional memory savings via subsequence entropy encoding. We observe that several quantization granularities are can be applied to the KV cache tensor [context\_len, head\_num, head\_dim]. Inspired by KIVI [20], we partition the key (K) cache along the context\_len dimension into fixed-size blocks and apply channel-wise quantization within each block. For the value (V) cache, we adopt a token-wise quantization strategy.

**3.1.2 Entropy Encoding.** Following quantization, the histogram of integers reveals that the distribution of the quantized values is highly skewed, with most values concentrated around a few discrete levels, shown in figure 3. This redundancy makes Entropy Encoding an ideal option to further reduce data size. We propose to adopt Huffman-based encoding to encode the quantization codes. Compared to alternatives such as arithmetic encoding[35] or Asymmetric Numeral Systems (ANS)[7], Huffman-based encoding shows great balance between simplicity and efficiency for KV cache encoding based on our evaluation.

**3.1.3 Compression Design Trade-offs.** Based on our experiments, we acknowledge the effectiveness of adding a Lorenzo predictor before quantization to capture spatial information. However, to meet the performance requirements of large language model inference, we prioritize cache-resident decompression to accelerate the decoding process. Moreover, the computational patterns of the Lorenzo predictor and Huffman encoding direction conflict with each other. For K cache, the dot product computation in matrix-vector multiplication occurs along the head\_dim dimension, whereas the inverse operation of the Lorenzo predictor follows a sequential dependency in the vertical direction during decompression. Integrating pre-quantization predictors, entropy decoding, and matrix-vector multiplication into a unified pipeline requires allocating substantial shared memory per GPU thread block to serve as an intermediate buffer, which introduces significant overhead to the decompression process. As a result, we conclude that incorporating such predictors before quantization result in a computational cost that outweighs the marginal compression gains. By decompressing data directly into cache and feeding it immediately to the matrix-vector multiplication kernels, we eliminate the need to write decompressed data back to global memory and reduce memory access overhead where compressed data is significantly smaller than original.

### 3.2 Compression Design

In the prefill stage, the LLM processes a user prompt containing thousands of tokens, with each token generating a fixed-dimension vector (shape [head\_num, head\_dim]) per transformer layer. Across all layers, this results in layer\_num  $\times$  2 vectors (two per layer corresponding to the key and value caches). Due to statistical differences between layers, we generate shared Huffman codebooks for each layer during LLM inference prefill stage.

**3.2.1 Buffering and Blocking.** For both K and V cache, we maintain a buffer of shape [buffer\_ctx\_len, head\_num, head\_dim], where buffer\_ctx\_len ranges from 1 to buffer\_size. When the buffer overflows, it is truncated such that its size falls within the

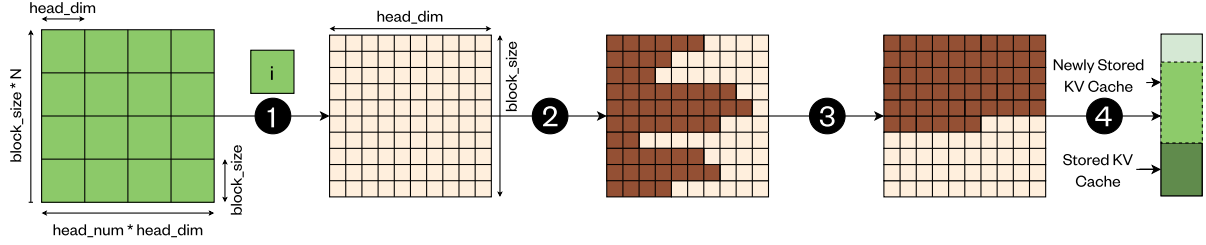


**Figure 4: Compression Overview.** 1. For each 2D block in the KV cache, assign a unique index that indicates the block’s position within the entire cache. 2. Each 2D block is loaded into shared memory in a coalesced manner. 3. According to the dot product direction, each vector is encoded into bits and stored in the thread’s shared memory buffer. 4. An in-block inclusive scan is performed to compute bit offsets for every thread, aggregating all bits into a contiguous chunk in shared memory. 5. The atomic offset is updated, and all threads coalescedly write the chunk back to global memory.

allowed range and can be partitioned into complete blocks. The overview of compression design shwon in the figure 4.

The K cache is considered as a tensor with shape  $[\text{context\_len}, \text{head\_num} \times \text{head\_dim}]$ . We map it to 2D blocks for compression. Since the matrix-vector multiplication dot product operates along the `head_dim` dimension, we must use `head_dim` as one of the dimensions of the 2D blocks when assign the buffer into complete blocks. The `context_len` is used as the other dimension of the 2D blocks, and the tensor is split into `head_num` parts.

For the V cache, the vector dot product in matrix-vector multiplication occurs along the `context_len` dimension, we divide the tensor to `head_dim` blocks (i.e., the same as K cache) to simplify the kernel implementation for the compression of both K and V caches.

**3.2.2 GPU-based Entropy Encoding.** Once blocked, the compression process is executed on the GPU and consists of the following six stages: **Coalesced Memory Loading:** The 2D block is loaded into shared memory. **Huffman-based Encoding:** Each thread compresses its assigned data slice of a row or column of the 2D data block in shared memory. Usually a `head_dim` length vector per thread. **Inclusive Scan:** An in-block inclusive scan computes bit offsets. **Data Aggregation:** Encoded data is aggregated in shared memory for coalesced global memory write-back. **Index Synchronization:** A wait-free, atomic operation synchronizes the global memory write-back index. **Coalesced Global Memory Write-back:** Compressed data is written back to global memory in a coalesced manner.

As shown in Figure 4, in stage 1 of the compression process, we assign a unique index to each 2D block in the overflowed, truncated KV cache chunk. This index identifies both the attention head to which the 2D block belongs and its corresponding `ctx_len` range. For each 2D block, we launch a GPU thread block containing `block_size` threads to perform compression. For K cache compression, threads within a block access contiguous memory addresses in the 2D block of shape  $[\text{block\_size}, \text{head\_dim}]$ , loading the data into shared memory. Within each GPU block, every thread is responsible for compressing one specific row of the K cache, each row having a shape of  $[\text{head\_dim}]$ . Similarly, for each V cache 2D block with shape  $[\text{head\_dim}, \text{block\_size}]$ , each thread processes a specific column, matching the shape of the K cache. In step 2, each thread then encodes one row or column of data in shared memory. To minimize bank conflicts, we set the shape of the shared

memory 2D block to ensure that both K and V compressions can access shared memory efficiently. Prior to the encoding process, the shared Huffman codebooks is loaded into shared memory to enable efficient encoding.

Once all threads have finished encoding, in step 3, the bit counts produced during entropy encoding are accumulated. Each thread within the block performs an inclusive scan using the CUB library to determine its bit offset within the aggregate buffer. After obtaining the total bit count, each thread writes its compressed bits to a shared memory buffer for aggregation. In the final step 4, the block performs a global atomic operation that updates a global variable to acquire the latest available index for writing the compressed data to global memory. This is followed by a coalesced write of the compressed data to GPU global memory. The atomic operation is crucial for preventing write-back conflicts between GPU thread blocks—without it, two thread blocks might retrieve and update the global offset variable simultaneously, leading to data being written to the same address and resulting in decompression errors.

Our 2D blockwise compression design is highly flexible and readily integrates with mainstream inference frameworks such as vLLM[15] and SGLang[38], both of which employ block-wise KV cache management strategies. Additionally, our framework can easily extend to other encoding algorithms, which can efficiently process `head_dim` unsigned 8-bit integers. For example, our framework can be adapted to encoding methods such as FSE[5], Bitshuffle[21, 36], and fixed-length encoding[11].

Although our parallel approach enables fine-grained Huffman encoding, it introduces memory overhead from additional metadata. Specifically, each thread needs an unsigned 16-bit integer to store the number of bits generated during encoding, while each block requires an unsigned 32-bit integer to store the global memory index for the compressed data. Given the average number of bits per encoded unsigned 8-bit integer is approximately 2, the total memory overhead for thread metadata is  $16/(\text{head\_dim} \times \text{avg\_bits\_per\_integer})$ , which corresponds to approximately  $\frac{1}{16}$  of the compressed data size, or  $\frac{1}{128}$  of the original data size. The per-block 32-bit integer used for the global memory index is even less significant, contributing less than  $\frac{1}{16}$  of the compressed data size. Therefore, the overall memory overhead for metadata is negligible compared to the size of the compressed data.

**3.2.3 Natural Data Appending.** During the decoding stage of LLM inference, each decoding step produces a new cache vector of shape  $[\text{head\_num}, \text{head\_dim}]$ , with the entire KV cache for a given layer participating in the attention computation. We propose to preallocate a buffer that can accommodate up to `buffer_size` newly generated cache vectors. The buffer is truncated only when the number of cache vectors exceeds `buffer_size`, ensuring efficient and consistent data management.

Each newly generated 2D block receives a unique block index that continues from the last used index in the compression sequence. These new cache vectors are then compressed using our encoding kernel. The compressed data for each 2D block remains independent due to our blockwise compression design, allowing us to seamlessly append the newly compressed data to the end of the existing compressed data buffer to allow efficient storage and effective management of the compressed cache over time.

In practice, repeated kernel launches on GPUs can introduce substantial performance overhead and limit maximum throughput due to high launch latency. For example, in LLaMA2-13B inference with a context length of 32K, block size of 64, and 512 separate kernel launches, the cumulative launch time limits throughput to approximately 61 GB/s. To address this, we employ a single kernel launch with multiple parallel GPU blocks to decode compressed data concurrently, effectively minimizing the overhead associated with frequent kernel invocations during decoding.

### 3.3 Decompression Design

During the decode stage of LLM inference, each iteration compresses the KV cache of only one input token while requiring decompression of the entire contextual KV cache. This creates a significant **imbalance** in the demand for compression versus decompression operations. Therefore, in our evaluation and performance optimization, we focus primarily on decompression throughput.

**3.3.1 High-throughput GPU Decoding.** One of the major bottlenecks in decompression is Huffman-based decoding coupled with the global memory write-back of decompressed data. To mitigate this, we redesign the decoding process to improve the decompression efficiency. One of the classic GPU Huffman decoding implementations is from cuSZ[31]. However, cuSZ adopts a coarse-grained block partitioning strategy that limits the achievable parallelism during decompression. Moreover, its bitwise decoding involves frequent if-else branching within the decoding loop for each bit, resulting in excessive thread divergence and underutilization of GPU resources. In comparison, our solution adopt fine-grained parallel encoding that achieves around 256 bits of decoding per thread, which can even reduce to 128 bits considering that the meta data overhead is negligible.

To address the branch divergence issue due to the fact that all threads within a warp execute the same instruction simultaneously on GPUs, we redesign the decoding process to improve its efficiency. We consider Huffman-based decoding as a tree traversal. Starting at the root of the tree, we update a pointer instead of using explicit conditional statements to navigate toward the leaf nodes. Specifically, we propose two major optimizations:

**Array-Based Representation of the Huffman Tree:** Due to the frequent access requirements of the Huffman decode tree,

we must store the codebook in GPU shared memory to achieve high-speed access, which requires a compact representation of the Huffman tree. To efficiently store a binary tree in contiguous memory, we arrange the Huffman tree nodes adjacent to one another. In this representation, traditional pointers in each node are replaced by indexes that reference the node's position in the node array. Each parent node contains two indexes representing references to its child nodes.

**Branch Divergence-Free Approach:** Rather than using explicit conditional statements to navigate the Huffman tree, we employ branchless operations for decoding to minimize branch divergence in parallel environments. Specifically, during tree traversal, each internal node stores its child node indexes in a two-element array, and the bit value from the bit stream is used directly as the index to select the next node—if the bit is 0, traversal proceeds to `indexes[0]`; if it is 1, to `indexes[1]`. For symbol handling, two key optimizations are applied: First, at each iteration, the symbol from the current node is always written to the decode buffer, but the buffer's write position is only advanced when the node represents a symbol. This is achieved by updating the write index using `write_idx+ = nodes[index].is_symbol`, so that only symbol nodes increment the output position. Second, returning to the root node after decoding a symbol is implemented with bitwise logic: the tree position is reset by computing `index& =~ (-nodes[index].is_symbol)`, which sets `index` to 0 if the current node is a symbol node (`is_symbol = 1`), and leaves `index` unchanged otherwise (`is_symbol = 0`). By avoiding all conditional branches inside the decoding loop, our approach achieves substantial reductions in branch divergence and improve efficiency for parallel decoders. The decoding process iterates over the bit stream, using each bit to select the next node in the tree and applying these branchless updates, until all bits have been processed.

**3.3.2 Cache-Resident Decompression.** We propose to performing decompression directly in cache and consuming the data *in situ*, thereby avoiding the need to write the decompressed output back to global memory. Since the KV cache is used for matrix-vector multiplication during the computation of attention weights and outputs, we are able to execute this multiplication operation directly on data stored in cache. Our 2D blockwise compression and decompression approach, combined with carefully chosen encoding strategies, ensures that decompressed data is immediately available as input for subsequent matrix-vector multiplication operations.

For the K cache with 2D block  $[\text{block\_size}, \text{head\_dim}]$ , each head's Q vector performs a dot product with the corresponding head's K vector. By assigning each thread to process a particular  $[\text{head\_dim}]$  row within the 2D block, we can directly decompress the vector for a given head in K and immediately accumulate the dot product result using the decompressed data.

For the V cache with 2D block  $[\text{head\_dim}, \text{block\_size}]$ , the attention weights of shape  $[\text{context\_length}, \text{head\_num}]$  are multiplied by the vectors for each head in V. We assign each thread to a particular  $[\text{head\_dim}]$  row of the 2D block, enabling direct decompression of the vectors for specific heads in V and immediate use for dot product accumulation. After fusing the decompression and matrix-vector multiplication kernels, we obtain a matrix of shape  $[\text{context\_length} / \text{head\_num}, \text{head\_num}]$ . The final step

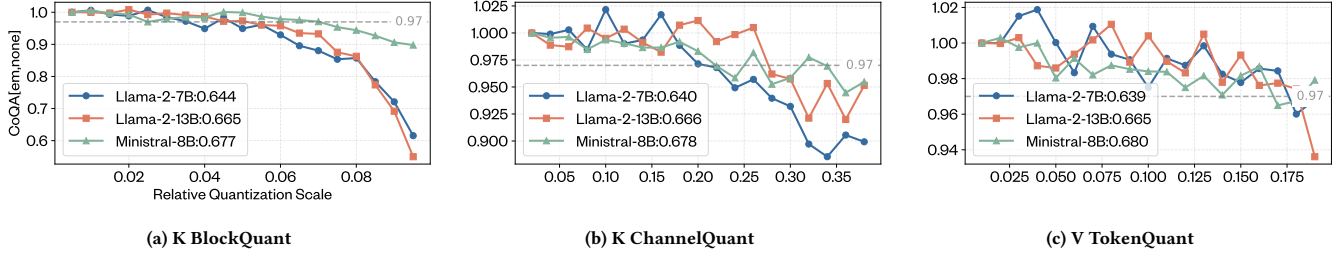


**Figure 5: Accuracy(Normalized, CoQA[em,none]) vs KV standalone Relative quantization scale from three models. The numbers to the right of the legend show the value that corresponds to the normalized value of 1 for each model.**

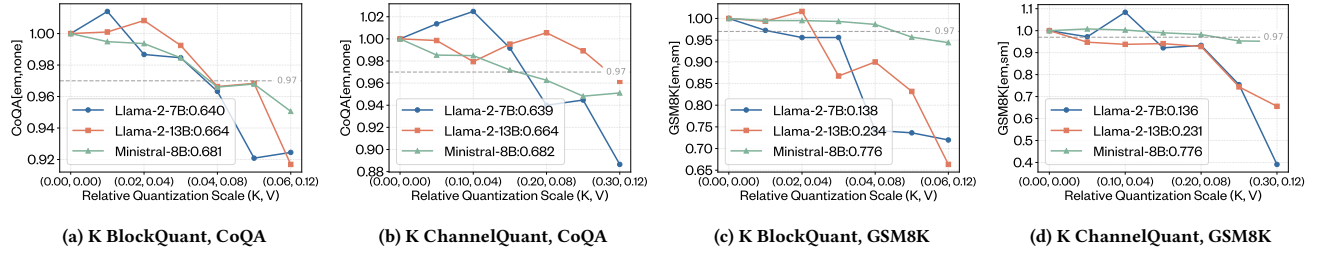


**Figure 6: Accuracy(Normalized, CoQA[em,none], GSM8K[em,sm]) vs Relative quantization scale([K,V]) from three models. The numbers to the right of the legend show the value that corresponds to the normalized value of 1 for each model.**

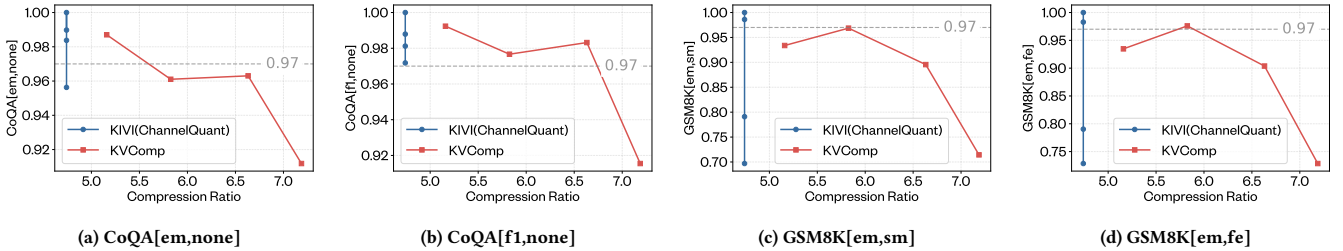


**Figure 7: Accuracy (Normalized, CoQA [EM, none], GSM8K [EM, SM]) versus relative quantization scale ([K, V]) for Llama2-13B. The reason the KIVI curve is vertical with respect to the x-axis is that, although the quantization scale is varied, the bit-width used to represent each data point can only be an integer; thus, the compression ratio remains unchanged.**

is a sum reduction, which incurs minimal computational overhead and produces the final result.

## 4 Evaluation

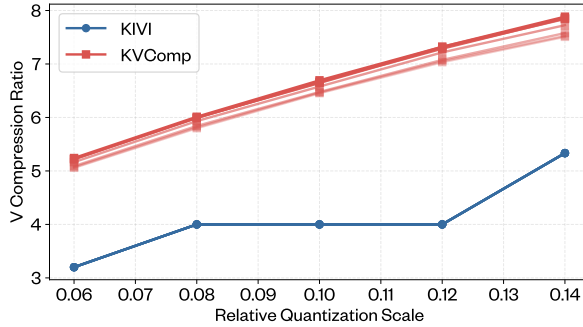
### 4.1 Experiment Setup

The experiments are based on two systems. The first cluster features nodes equipped with two Intel Xeon E5-2620v4 processors, offering 16 physical cores in total, along with four NVIDIA Tesla V100 GPUs per node. The second workstation equipped with a single AMD Ryzen Threadripper 7970X CPU (32 physical cores), 256 GB RAM, and two NVIDIA GeForce RTX 4090 GPUs (24 GB each).

We select the model accuracy, compression ratio, and decompression throughput as our metrics. Specifically, we selected three models (i.e., Llama2 7B, Llama2 13B, and Minstral 8B) and two benchmarks (i.e., CoQA and GSM8K), to evaluate model accuracy in different configurations. Although our solution can maintain the same accuracy as the standalone quantization methods, we discovered an more suitable quantization granularity for our method

that achieves higher compression ratios while preserving model accuracy. Due to the asymmetric nature of compression and decompression demands in our use case, we focus primarily on decompression throughput. We compare the throughput of our cache-resident decompression method with the original standalone decompressor.

We use KIVI [20] quantization as the baseline for evaluating model accuracy and compression ratio. The original data type of the KV cache is float16, existing lossy compressors do not natively support this format. Furthermore, no current lossy compressors support fine-grained quantization or handle dynamically growing data structures efficiently. We also acknowledge that our solution is orthogonal to KV cache pruning and GPU-CPU migration, and can be combined with these methods for further optimization. For decompression throughput, we use our in-house standalone compressor implementation as the baseline. We also include raw cuBLAS matrix vector multiplication throughput in our comparison.



(a) V TokenQuant

**Figure 8: V Compression Ratio comparison between KIVI and KVComp across various relative quantization scales. Lines correspond to different context lengths (ctx\_len) [2048-16384], where darker shades indicate larger ctx\_len values.**

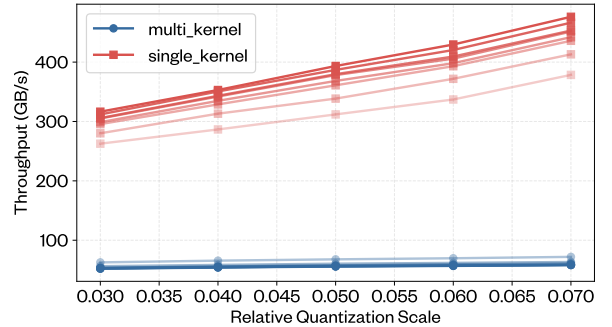
## 4.2 Model Accuracy vs Compression Ratio

Based on the HuggingFace **transformers** Python package, we implemented a **KVCompCache** class, which provides the required interface functions for the **Cache** class and can be efficiently integrated with all supported models.

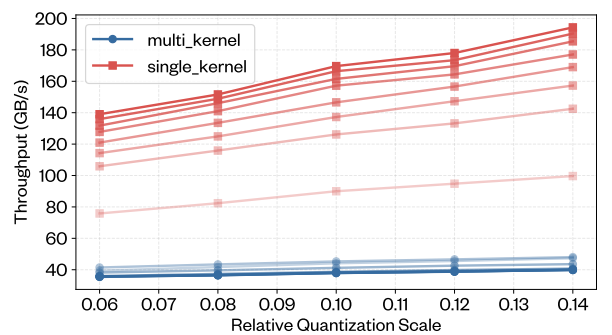
Our compression configuration includes three key parameters:

- **Block size**: the size of each block of the K cache that is truncated from the buffer when it overflows
- **Maximum buffer size**: the upper limit for the cache buffer.
- **Relative quantization scale**: the relative scaling factor applied during quantization within each block. Specifically, we define a global relative quantization scale between [0, 1]. The actual quantization scale for each block/channel is  $rel\_quant\_scale * (max\_value - min\_value)$ .

**4.2.1 K and V Standalone Test.** First, we conduct standalone accuracy benchmarks for K and V, varying relative quantization scales to identify the turning point at which accuracy drops significantly, shown in Figure 5. During this experiment, we only compress K with original V, or compress V with original K to determine their standalone impact to model accuracy. For K, we conduct both Block-Quant and ChannelQuant for comparison, where ChannelQuant is a similar quantization solution compared to KIVI. For V, we only conduct TokenQuant as it already align with our decompression design. We normalize the original model accuracy to 1 and unify all accuracy values accordingly for simplicity. We select the largest quantization relative scale at which the model’s accuracy drops by less than 3%. We choose 3% because model accuracy drop dramatically if the accuracy drop below 97% shown in the K and V standalone accuracy test. Note that although the corresponding *rel\_quant\_scale* of the turning point of K ChannelQuant is larger than that of K BlockQuant, they are not directly comparable due to their different value range. We will directly compare the two strategies by their compression ratios in Figure 7. Based on Figure 5, the accuracy turning point for the K BlockQuant quantization scale is approximately 0.05–0.06. For K ChannelQuant, the turning point can be set around 0.25–0.3. For V TokenQuant, the turning point occurs at approximately 0.15–0.2.



(a) K decompression throughput



(b) V decompression throughput

**Figure 9: Decompression throughput single kernel (decompress + matrix vector multiplication) vs multi kernels (huffman decode + dequantization + matrix vector multiplication). Lines correspond to different context lengths (ctx\_len) [2048-16384], where darker shades indicate larger ctx\_len values.**

**4.2.2 K and V Combined Test.** In this subsection, we introduced a more comprehensive benchmark, GSM8K, to assess the model accuracy drop with both compressed K and V. We fix the ratio of *rel\_quant\_scale* of K and *rel\_quant\_scale* of V based on the turning points from Figure 5, and conduct our experiments with both K and V compressed, shown in Figure 6. We can observe that even with different LLM model size and LLM model structure (i.e., Llama2 7B, Llama2 13B, and Minstral 8B), our solution select consistent *rel\_quant\_scale* given a benchmark.

Furthermore, we conducted experiments to measure the compression ratios with our solution compared to KIVI. For the compression ratio tests, we used text from the WikiText-103-v1 dataset, assembling contexts from its lines and using this text as model input to generate the KV cache.

For K quantization, we established the relationship between compression ratio and accuracy, as shown in Figure 7. Overall, our method improves the compression ratio by up to 41% and on average 32% compared to KIVI with no/minimum accuracy degradation. For V quantization, since Token-wise quantization is also used in KIVI, we focused on the compression ratio improvement from our entropy encoding solution, as shown in Figure 8. We evaluate the compression ratio across different context lengths, ranging

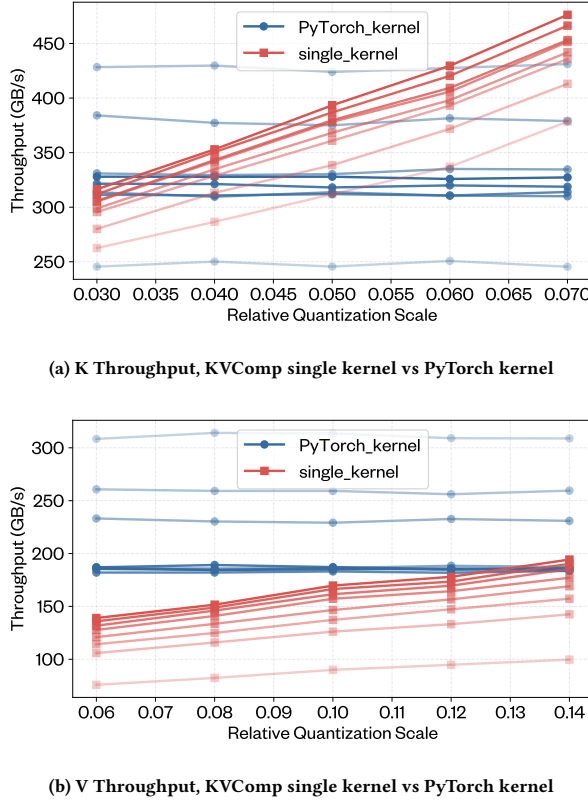


**Figure 10: Decompression throughput KVComp single kernel (decompress + matrix vector multiplication) vs PyTorch kernels (matrix vector multiplication only). Lines correspond to different context lengths (ctx\_len) [2048-16384], where darker shades indicate larger ctx\_len values.**

from 4,096 to 16,384. Our method achieves up to 83% (i.e., Relative quantization scale = 0.12, Context length = 16384) and on average 62% improvement over KIVI in compression ratio while maintaining the same model accuracy. Additionally, we observe that our solution achieves a consistent compression ratio across different context length scales, indicating that it scales effectively in large context length scenarios.

### 4.3 Inference Computation Throughput

As discussed in Section 3.3, during the decoding stage of LLM inference, each iteration requires compressing the KV cache corresponding to a single input token but decompressing the entire KV cache for the context. This results in a significant imbalance between compression and decompression demands. Consequently, we focus on decompression throughput and the corresponding inference computation throughput in our evaluation.

We use the optimal compression configurations identified in previous analyses, and collect KV cache data during model inference. We then record both CUDA kernel execution times and the sizes of original and compressed data from compressing and decompressing KV cache data during inference. For standalone decompression

kernels, we measured the execution times for Huffman-based decoding, dequantization and matrix-vector multiplication. For the cache-resident decompression kernel, we measured the execution time of our fused (i.e., decompression + matrix-vector multiplication) kernel. First, we compare the kernel times of the multi-kernel and single-kernel implementations; then, we compare our single fused kernel (decompression + matrix vector multiplication) with the cuBLAS-based matrix-vector multiplication kernel.

Figure 9 presents the kernel execution times comparison between our single-kernel implementation and the multi-kernel pipeline. As the relative quantization scale increases, the kernel execution time decreases. This is because a larger quantization scale correlate to a higher compression ratio, thus a smaller bits/value KV cache size. Since our decode algorithm processes only one bit per decoding iteration, having fewer bits to decode results in faster decompression. Our solution outperforms the multi-kernel implementation in all scenarios. Additionally, we observe that our solution can provide extremely high throughput of over 400 GB/s for K and over 180 GB/s for V. Note that this high-throughput single kernel not only include the decompression for KV cache, but also their subsequent matrix multiplication operations.

Next, we compare the kernel execution time of our single-kernel implementation with that of the cuBLAS-based matrix-vector multiplication kernel, as shown in Figure 10. It is important to note that this comparison is not strictly fair, as the cuBLAS kernel performs only matrix multiplication, whereas our kernel includes both decompression and matrix-vector multiplication. However, as the context length increases, our kernel outperforms cuBLAS—even while performing additional work. This is primarily because our approach not only keeps data in situ during decompression and computation, avoiding intermediate memory transfers, but also operates on compressed data that loads significantly less data from global memory compared to loading original data by cuBLAS. This reduction in data movement becomes substantial at high compression ratios, enabling our fused kernel to surpass cuBLAS in overall performance. In addition, shown in Figure 10, our solution scales well with increasing context length. We observe a clear performance improvement as the context length grows, which is mainly due to higher hardware utilization when processing larger volumes of data.

Lastly, we compute the equivalent decompression throughput of our single-kernel design by analyzing its performance difference relative to cuBLAS, as shown in Figure 11. We observe that once the context length exceeds 8,192, the equivalent decompression throughput of our kernel becomes significantly higher than that of standalone matrix multiplication. This indicates that in real-world scenarios with long context lengths, our approach introduces negligible performance overhead—or even yields performance gains—while simultaneously providing high compression ratios for substantial memory reduction.

## 5 Conclusion and Future Work

In this paper, we introduce KVComp, a high-performance, LLM-aware lossy compression framework designed to address the growing memory bottleneck posed by the KV cache during LLM inference. By combining fine-grained quantization with GPU-optimized

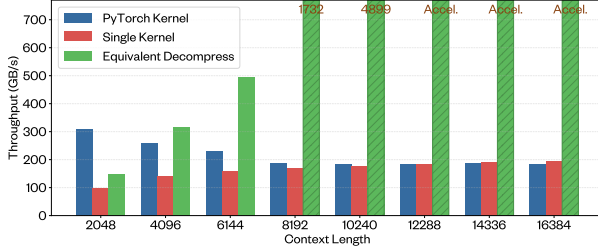


**Figure 11: V cache, Single kernel (decompress + matrix-vector multiplication), PyTorch kernel, and equivalent decompress.** As the context length increases, our single kernel throughput continues to improve, eventually accelerating the matrix-vector multiplication operation, which is typically memory-bound. Thus, lossy compression techniques can not only reduce data size but also enhance computational performance.

Huffman-based encoding and cache-resident decompression, KVComp significantly reduces the memory footprint of the KV cache while preserving model accuracy and achieving high execution efficiency. KVComp achieves up to 83% improvement in compression ratio, with no additional accuracy degradation. KVComp also introduce little overhead, or in some cases, faster execution than cuBLAS-based attention kernels due to less data movement.

In the future, we plan to investigate more efficient entropy encoding techniques to further improve both compression ratio and throughput. Additionally, we will extend our solution to a wider range of benchmarks and models.

## References

- [1] Josh Achiam, Steven Adler, Sandhini Agarwal, Lama Ahmad, Ilge Akkaya, Florencia Leoni Aleman, Diogo Almeida, Janko Alten Schmidt, Sam Altman, Shyam Anadkat, et al. 2023. Gpt-4 technical report. *arXiv preprint arXiv:2303.08774* (2023).
- [2] Amey Agrawal, Ashish Panwar, Jayashree Mohan, Nipun Kwatra, Bhargav S Gulavani, and Ramachandran Ramjee. 2023. Sarathi: Efficient llm inference by piggybacking decodes with chunked prefills. *arXiv preprint arXiv:2308.16369* (2023).
- [3] Ron Banner, Yury Nahshan, and Daniel Soudry. 2019. Post training 4-bit quantization of convolutional networks for rapid-deployment. *Advances in Neural Information Processing Systems* 32 (2019).
- [4] Tom Brown, Benjamin Mann, Nick Ryder, Melanie Subbiah, Jared D Kaplan, Prafulla Dhariwal, Arvind Neelakantan, Pranav Shyam, Girish Sastry, Amanda Askell, et al. 2020. Language models are few-shot learners. *Advances in neural information processing systems* 33 (2020), 1877–1901.
- [5] Cyan (Yann Collet). 2013. Finite State Entropy – A new breed of entropy coder. [urlhttps://fastcompression.blogspot.com/2013/12/finite-state-entropy-new-breed-of.html](https://fastcompression.blogspot.com/2013/12/finite-state-entropy-new-breed-of.html). RealTime Data Compression blog post.
- [6] Sheng Di and Franck Cappello. 2016. Fast error-bounded lossy HPC data compression with SZ. In *2016 ieee international parallel and distributed processing symposium (ipdps)*. IEEE, 730–739.
- [7] Jarek Duda. 2009. Asymmetric numeral systems. *arXiv preprint arXiv:0902.0271* (2009).
- [8] Elias Frantar, Saleh Ashkboos, Torsten Hoefer, and Dan Alistarh. 2022. Gptq: Accurate post-training quantization for generative pre-trained transformers. *arXiv preprint arXiv:2210.17323* (2022).
- [9] Song Han, Huizi Mao, and William J. Dally. 2016. Deep Compression: Compressing Deep Neural Networks with Pruning, Trained Quantization and Huffman Coding. In *4th International Conference on Learning Representations (ICLR)*. <https://arxiv.org/abs/1510.00149>
- [10] Coleman Hooper, Sehoon Kim, Hiva Mohammazadeh, Michael W Mahoney, Sophia Shao, Kurt Keutzer, and Amir Gholami. 2024. Kvquant: Towards 10 million context length llm inference with kv cache quantization. *Advances in Neural Information Processing Systems* 37 (2024), 1270–1303.
- [11] Yafan Huang, Sheng Di, Xiaodong Yu, Guanpeng Li, and Franck Cappello. 2023. cuszp: An ultra-fast gpu error-bounded lossy compression framework with optimized end-to-end performance. In *Proceedings of the International Conference for High Performance Computing, Networking, Storage and Analysis*. 1–13.
- [12] Benoit Jacob, Skirmantas Kligys, Bo Chen, Menglong Zhu, Matthew Tang, Andrew Howard, Hartwig Adam, and Dmitry Kalenichenko. 2018. Quantization and training of neural networks for efficient integer-arithmetic-only inference. In *Proceedings of the IEEE conference on computer vision and pattern recognition*. 2704–2713.
- [13] Sian Jin, Sheng Di, Xin Liang, Jiannan Tian, Dingwen Tao, and Franck Cappello. 2019. DeepSZ: A novel framework to compress deep neural networks by using error-bounded lossy compression. In *Proceedings of the 28th international symposium on high-performance parallel and distributed computing*. 159–170.
- [14] Sian Jin, Chengming Zhang, Xintong Jiang, Yunhe Feng, Hui Guan, Guanpeng Li, Shuaiwen Leon Song, and Dingwen Tao. 2021. Comet: a novel memory-efficient deep learning training framework by using error-bounded lossy compression. *arXiv preprint arXiv:2111.09562* (2021).
- [15] Woosuk Kwon, Zhuohan Li, Siyuan Zhuang, Ying Sheng, Lianmin Zheng, Cody Hao Yu, Joseph Gonzalez, Hao Zhang, and Ion Stoica. 2023. Efficient memory management for large language model serving with paginated attention. In *Proceedings of the 29th Symposium on Operating Systems Principles*. 611–626.
- [16] Xin Liang, Sheng Di, Dingwen Tao, Sihuan Li, Shaomeng Li, Hanqi Guo, Zizhong Chen, and Franck Cappello. 2018. Error-controlled lossy compression optimized for high compression ratios of scientific datasets. In *2018 IEEE International Conference on Big Data*. IEEE, 438–447.
- [17] Peter Lindstrom. 2014. Fixed-rate compressed floating-point arrays. *IEEE transactions on visualization and computer graphics* 20, 12 (2014), 2674–2683.
- [18] Yuhai Liu, Hanchen Li, Yihua Cheng, Siddhant Ray, Yuyang Huang, Qizheng Zhang, Kuntai Du, Jiayi Yao, Shan Lu, Ganesh Ananthanarayanan, et al. 2024. Cachegeen: Kv cache compression and streaming for fast large language model serving. In *Proceedings of the ACM SIGCOMM 2024 Conference*. 38–56.
- [19] Zichang Liu, Aditya Desai, Fangshuo Liao, Weitao Wang, Victor Xie, Zhaozhuo Xu, Anastasios Kyriolidis, and Anshumali Shrivastava. 2023. Scissorhands: Exploiting the persistence of importance hypothesis for llm kv cache compression at test time. *Advances in Neural Information Processing Systems* 36 (2023), 52342–52364.
- [20] Zirui Liu, Jiayi Yuan, Hongye Jin, Shaochen Zhong, Zhaozhuo Xu, Vladimir Braverman, Beidi Chen, and Xia Hu. 2024. Kivi: A tuning-free asymmetric 2bit quantization for kv cache. *arXiv preprint arXiv:2402.02750* (2024).
- [21] Kiyoshi Masui, Mandana Amiri, Liam Connor, Meiling Deng, Mateus Fandino, Carolin Höfer, Mark Halpern, David Hanna, Adam D Hincks, Gary Hinshaw, et al. 2015. A compression scheme for radio data in high performance computing. *Astronomy and Computing* 12 (2015), 181–190.

- [22] Xinxin Mei and Xiaowen Chu. 2016. Dissecting GPU memory hierarchy through microbenchmarking. *IEEE Transactions on Parallel and Distributed Systems* 28, 1 (2016), 72–86.
- [23] Jens-Rainer Ohm, Gary J Sullivan, Heiko Schwarz, Thio Keng Tan, and Thomas Wiegand. 2012. Comparison of the coding efficiency of video coding standards—including high efficiency video coding (HEVC). *IEEE Transactions on circuits and systems for video technology* 22, 12 (2012), 1669–1684.
- [24] Reiner Pope, Sholto Douglas, Aakanksha Chowdhery, Jacob Devlin, James Bradbury, Jonathan Heek, Kefan Xiao, Shivani Agrawal, and Jeff Dean. 2023. Efficiently scaling transformer inference. *Proceedings of Machine Learning and Systems* 5 (2023), 606–624.
- [25] Alec Radford, Karthik Narasimhan, Tim Salimans, Ilya Sutskever, et al. 2018. Improving language understanding by generative pre-training. (2018).
- [26] Noam Shazeer. 2019. Fast transformer decoding: One write-head is all you need. *arXiv preprint arXiv:1911.02150* (2019).
- [27] Ying Sheng, Lianmin Zheng, Binhang Yuan, Zhuohan Li, Max Ryabinin, Beidi Chen, Percy Liang, Christopher Ré, Ion Stoica, and Ce Zhang. 2023. Flexgen: High-throughput generative inference of large language models with a single gpu. In *International Conference on Machine Learning*. PMLR, 31094–31116.
- [28] Dingwen Tao, Sheng Di, Zizhong Chen, and Franck Cappello. 2017. Significantly improving lossy compression for scientific data sets based on multidimensional prediction and error-controlled quantization. In *2017 IEEE International Parallel and Distributed Processing Symposium*. IEEE, 1129–1139.
- [29] David Taubman, Erik Ordentlich, Marcelo Weinberger, and Gadiel Seroussi. 2002. Embedded block coding in JPEG 2000. *Signal Processing: Image Communication* 17, 1 (2002), 49–72.
- [30] Ross Taylor, Marcin Kardas, Guillem Cucurull, Thomas Scialom, Anthony Hartshorn, Elvis Saravia, Andrew Poulton, Viktor Kerkez, and Robert Stojnic. 2022. Galactica: A large language model for science. *arXiv preprint arXiv:2211.09085* (2022).
- [31] Jiannan Tian, Sheng Di, Kai Zhao, Cody Rivera, Megan Hickman Fulp, Robert Underwood, Sian Jin, Xin Liang, Jon Calhoun, Dingwen Tao, et al. 2020. Cusz: An efficient gpu-based error-bounded lossy compression framework for scientific data. In *Proceedings of the ACM International Conference on Parallel Architectures and Compilation Techniques*. 3–15.
- [32] Ashish Vaswani, Noam Shazeer, Niki Parmar, Jakob Uszkoreit, Llion Jones, Aidan N Gomez, Łukasz Kaiser, and Illia Polosukhin. 2017. Attention is all you need. *Advances in neural information processing systems* 30 (2017).
- [33] Gregory K Wallace. 1992. The JPEG still picture compression standard. *IEEE transactions on consumer electronics* 38, 1 (1992), xviii–xxxiv.
- [34] Hanrui Wang, Zhekai Zhang, and Song Han. 2021. Spatten: Efficient sparse attention architecture with cascade token and head pruning. In *2021 IEEE International Symposium on High-Performance Computer Architecture (HPCA)*. IEEE, 97–110.
- [35] Ian H Witten, Radford M Neal, and John G Cleary. 1987. Arithmetic coding for data compression. *Commun. ACM* 30, 6 (1987), 520–540.
- [36] Boyuan Zhang, Jiannan Tian, Sheng Di, Xiaodong Yu, Yunhe Feng, Xin Liang, Dingwen Tao, and Franck Cappello. 2023. Fz-gpu: A fast and high-ratio lossy compressor for scientific computing applications on gpus. In *Proceedings of the 32nd International Symposium on High-Performance Parallel and Distributed Computing*. 129–142.
- [37] Zhenyu Zhang, Shiwei Liu, Runjin Chen, Bhavya Kailkhura, Beidi Chen, and Atlas Wang. 2024. Q-hitter: A better token oracle for efficient llm inference via sparse-quantized kv cache. *Proceedings of Machine Learning and Systems* 6 (2024), 381–394.
- [38] Lianmin Zheng, Liangsheng Yin, Zhiqiang Xie, Chuyue Livia Sun, Jeff Huang, Cody Hao Yu, Shiyi Cao, Christos Kozyrakis, Ion Stoica, Joseph E Gonzalez, et al. 2024. Sglang: Efficient execution of structured language model programs. *Advances in Neural Information Processing Systems* 37 (2024), 62557–62583.